

Complexity in Hamiltonian-driven dissipative chaotic dynamical systems

Ying-Cheng Lai* and Celso Grebogi†

Institute for Plasma Research, University of Maryland, College Park, Maryland 20742

(Received 24 June 1996)

The existence of symmetry in chaotic dynamical systems often leads to one or several low-dimensional invariant subspaces in the phase space. We demonstrate that complex behaviors can arise when the dynamics in the invariant subspace is Hamiltonian but the full system is dissipative. In particular, an infinite number of distinct attractors can coexist. These attractors can be quasiperiodic, strange nonchaotic, and chaotic with different positive Lyapunov exponents. Finite perturbations in initial conditions or parameters can lead to a change from nonchaotic attractors to chaotic attractors. However, arbitrarily small perturbations can lead to dynamically distinct chaotic attractors. This work demonstrates that the interplay between conservative and dissipative dynamics can give rise to rich complexity even in physical systems with a few degrees of freedom. [S1063-651X(96)05311-1]

PACS number(s): 05.45.+b

I. INTRODUCTION

The study of complexity has been an area of growing recent interest [1–5]. Complex systems are characterized by three properties: (i) A complex system consists of many components that are interconnected in a complicated manner, (ii) the components of a complex system can be either regular or irregular, and (iii) the components exist on different length and/or time scales, i.e., a complex system exhibits a hierarchy of structures. These are also the *three traits* characterizing a complex system [1–5]. Complex systems arise in many different fields such as physics, chemistry, fluid mechanics, biology, economics, and computer science. Some specific examples are Rayleigh-Bénard convection [6], neuronal activity [7], extended nonlinear optical systems [8], and fluid beds [9]. Because of the hierarchical structure of a complex system, the state of the system can “hop” between different components when small perturbations are applied to the system or when the system is in a noisy environment. Thus one can control the behavior of a complex system to achieve desirable system performance by using small feedback perturbations to an accessible parameter or state of the system [5].

Complexity can arise in systems with few degrees of freedom. For instance, the double rotor map derived from a mechanical system of two degrees of freedom under external periodic kick [10] exhibits all three traits of a complex system in wide parameter ranges [5]. Often there are many coexisting periodic attractors whose basins of attraction are interconnected via unstable chaotic saddles in the basin boundaries in a very complicated manner. More recently, it has been demonstrated that the standard map, which describes the dynamics of a periodically kicked rotor (one and

a half degrees of freedom), can exhibit a huge number of coexisting periodic attractors when there is a weak dissipation in the system [11]. The basins of the mostly periodic attractors are interwoven in a complex way and the basin boundaries permeate most of the phase space. As a practical consequence of these complicated basin structures, the final asymptotic state of the system for a given initial condition and a given parameter set cannot be predicted reliably [12].

In the study of complex systems, it is important to be able to understand how complexity arises so that one may have a better understanding and thus be better able to control and manipulate the system. In particular, one wishes to establish the *fundamental link* between the intrinsic properties of the nonlinear dynamical systems and the observed complex behavior. In this regard, the study of complexity in low-dimensional dynamical systems is appealing because these systems are more accessible to understanding due to the success of low-dimensional chaos theory [13]. The purpose of this paper is to introduce a class of low-dimensional dynamical systems that exhibit extremely rich complex behavior and to understand the complexity in terms of the nonlinear dynamics of the system. In particular, we study dynamical systems with a simple kind of symmetry. The existence of symmetry often leads to low-dimensional invariant subspaces in the full phase space. We demonstrate that complexity can arise when the dynamics in the invariant subspace is conservative (Hamiltonian), but the full system is dissipative. We call such systems *Hamiltonian-driven dissipative dynamical systems*. For such a system, an infinite number of distinct attractors coexist. These attractors can be quasiperiodic, strange nonchaotic, or chaotic with different positive Lyapunov exponents. Finite perturbations in initial conditions or parameters can lead to change from quasiperiodic or strange nonchaotic attractors to chaotic attractors. However, arbitrarily small perturbations can lead to dynamically distinct chaotic attractors. The main point of the paper is that the interplay between conservative and dissipative dynamics can give rise to extremely rich complexity even when the system is low dimensional.

The paper is organized as follows. In Sec. II, we give a general argument that Hamiltonian-driven dissipative dy-

*Permanent address: Departments of Physics and Astronomy and of Mathematics, University of Kansas, Lawrence, KS 66045. Electronic address: lai@poincare.math.ukans.edu

†Also at Department of Mathematics, Institute for Physical Science and Technology, University of Maryland, College Park, MD 20742.

namical systems can generate rich complex behavior in the form of a hierarchy of qualitatively distinct attractors. This behavior fits the three traits characterizing a complex system. In Sec. III, we give a numerical example described by a three-dimensional map. In Sec. IV, we characterize the degree of unpredictability upon small perturbations by using the uncertainty exponent [12]. In Sec. V, we present a discussion.

II. HAMILTONIAN-DRIVEN DISSIPATIVE DYNAMICAL SYSTEMS

We consider dynamical systems with a low-dimensional invariant subspace denoted by \mathbf{S} . Since \mathbf{S} is invariant, initial conditions in \mathbf{S} result in trajectories that remain in \mathbf{S} forever. Now imagine that the dynamics in \mathbf{S} is conservative, mathematically described by Hamiltonian flows or area-preserving maps. Assume that ‘‘friction’’ occurs in the subspace \mathbf{T} that is transverse to \mathbf{S} . Thus the dynamics in the transverse subspace is dissipative and hence the full system is also dissipative. Specifically, we consider the following general class of N -dimensional discrete maps in \mathbb{R}^N ,

$$\begin{aligned} \mathbf{x}_{n+1} &= \mathbf{f}(\mathbf{x}_n), \\ \mathbf{y}_{n+1} &= F(\mathbf{x}_n, p)\mathbf{G}(\mathbf{y}_n), \end{aligned} \quad (1)$$

where $\mathbf{x} \in \mathbf{S} \subset \mathbb{R}^{N_S}$, $\mathbf{y} \in \mathbf{T} \subset \mathbb{R}^{N_T}$, $N_S \geq 1$, $N_T \geq 1$, $N_S + N_T = N$, and p is a parameter. The vector function $\mathbf{G}(\mathbf{y})$ possesses a certain symmetry, e.g., $\mathbf{G}(-\mathbf{y}) = -\mathbf{G}(\mathbf{y})$, so that $\mathbf{G}(\mathbf{0}) = \mathbf{0}$. The symmetric invariant subspace is then defined by $\mathbf{y} = \mathbf{0}$. We assume that both the \mathbf{x} and \mathbf{y} dynamics are bounded. The vector function $\mathbf{f}(\mathbf{x})$ is an area-preserving map that exhibits typical features of Hamiltonian phase space: the coexistence of the Kolmogorov-Arnold-Moser (KAM) tori and chaotic regions in wide parameter ranges [14]. The functions $F(\mathbf{x}_n, p)$ and $\mathbf{G}(\mathbf{y}_n)$ are chosen such that the magnitude of the determinant of the Jacobian matrix $|DJ_{\mathbf{y}}| \equiv |\partial \mathbf{y}_{n+1} / \partial \mathbf{y}_n|$ is less than one in some phase-space regions. For simplicity we assume that the system (1) has a skew-product structure, i.e., the \mathbf{x} dynamics is not influenced by the \mathbf{y} dynamics. Since $\mathbf{f}(\mathbf{x})$ is area preserving, the determinant of the Jacobian matrix of the full system Eq. (1) is determined solely by $DJ_{\mathbf{y}}$. Thus Eq. (1) is dissipative and the asymptotic sets of the system can be attractors. Since Eq. (1) has a skew-product structure, the attractors can be conveniently characterized by the largest Lyapunov exponents, denoted by Λ_S and Λ_T , for the invariant and transverse subspaces, respectively. Specifically, Λ_S and Λ_T are given by

$$\Lambda_S = \lim_{L \rightarrow \infty} \frac{1}{L} \sum_{n=1}^L \ln |\mathbf{Df}(\mathbf{x}_n) \cdot \mathbf{u}|, \quad (2)$$

$$\Lambda_T = \lim_{L \rightarrow \infty} \frac{1}{L} \sum_{n=1}^L \ln |F(\mathbf{x}_n, p) \mathbf{DG}(\mathbf{y}_n) \cdot \mathbf{v}|,$$

where $\mathbf{Df}(\mathbf{x}_n) \equiv \partial \mathbf{f}(\mathbf{x}_n) / \partial \mathbf{x}_n$, $\mathbf{DG}(\mathbf{y}_n) \equiv \partial \mathbf{G}(\mathbf{y}_n) / \partial \mathbf{y}_n$, and \mathbf{u} and \mathbf{v} are unit vectors in \mathbf{S} and \mathbf{T} , respectively. Another useful quantity is the transverse Lyapunov exponent Λ_{\perp} that characterizes the transverse stability for trajectories *restricted* to the invariant subspace \mathbf{S} [15]. It is given by

$$\Lambda_{\perp} = \lim_{L \rightarrow \infty} \frac{1}{L} \sum_{n=1}^L \ln |F(\mathbf{x}_n, p) \mathbf{DG}(\mathbf{0}) \cdot \mathbf{v}|, \quad (3)$$

where $\mathbf{DG}(\mathbf{0}) \equiv \partial \mathbf{G}(\mathbf{y}_n) / \partial \mathbf{y}_n|_{\mathbf{y}_n = \mathbf{0}}$ is evaluated at $\mathbf{y}_n = \mathbf{0}$. In general, if $\Lambda_{\perp} < 0$, then $\mathbf{y} = \mathbf{0}$ is asymptotically stable and hence $\Lambda_T = \Lambda_{\perp}$. However, $\Lambda_T \neq \Lambda_{\perp}$ if $\Lambda_{\perp} > 0$.

Under fairly general conditions, Eq. (1) can generate all three traits characterizing a complex system. This can be seen as follows. First, since $\mathbf{f}(\mathbf{x})$ is an area-preserving map, for typical parameter values there is apparently an infinite number of invariant sets in \mathbf{S} corresponding to chaotic sets and KAM surfaces (or tori) of different rotation numbers. We restrict our study to these parameter values. In such a case, different initial conditions \mathbf{x}_0 in \mathbf{S} yield different invariant measures. Notice that in Eq. (1), the \mathbf{x} dynamics can be regarded as the ‘‘driving’’ to the transverse \mathbf{y} dynamics. Thus different invariant measures in \mathbf{S} generate different driving and consequently generate distinct attracting motions in \mathbf{T} or distinct attractors in the full phase space. Depending on the parameters, attractors in the full phase space with a different number of positive Lyapunov exponents can be created by changing initial conditions. Since the KAM tori and the chaotic regions in \mathbf{S} are interconnected in a complicated way [14], we expect that the basins of the attraction for the attractors in the full phase space are also connected in a complex way. This is trait 1. Second, since there are both regular (KAM surfaces) and irregular (chaotic sets) components in \mathbf{S} , depending on the driving $\mathbf{F}(\mathbf{x}, p)$, the attractors can also be nonchaotic (ordered) with no positive Lyapunov exponent or chaotic (random) with one or several positive Lyapunov exponents. Small amount of noise can push a trajectory from one attractor to another. This is trait 2. Finally, it is known that KAM surfaces typically form a hierarchy of the so-called island-around-island structure [14] and hence the attractors in the full phase space are also organized in a hierarchy of structures. This is trait 3.

III. NUMERICAL EXAMPLE

We consider the three-dimensional version of Eq. (1),

$$\begin{aligned} x_{n+1} &= x_n + y_n, \quad \text{mod}(2\pi), \\ y_{n+1} &= y_n + k \sin(x_n + y_n), \quad \text{mod}(2\pi), \\ z_{n+1} &= \frac{1}{2\pi} (a \cos x_n + b \cos y_n + c) \sin(2\pi z_n), \end{aligned} \quad (4)$$

where k , a , b , and c are parameters. The invariant subspace is given by $z = 0$ and hence it is two dimensional. The dynamics in the invariant plane is conservative and it is that of a periodically kicked rotor (the standard map in x and y). The transverse subspace is one dimensional (in z) and bounded. The determinant of the Jacobian matrix of Eq. (4) is $|DJ| = (a \cos x_n + b \cos y_n + c) \cos(2\pi z_n)$, whose magnitude can be less than one in some phase-space regions. The system (4) is thus dissipative in these regions. We choose $k = 1$ in the standard map so that the invariant subspace contains both KAM surfaces and distinct chaotic regions. The transverse Lyapunov exponent Λ_{\perp} is given by

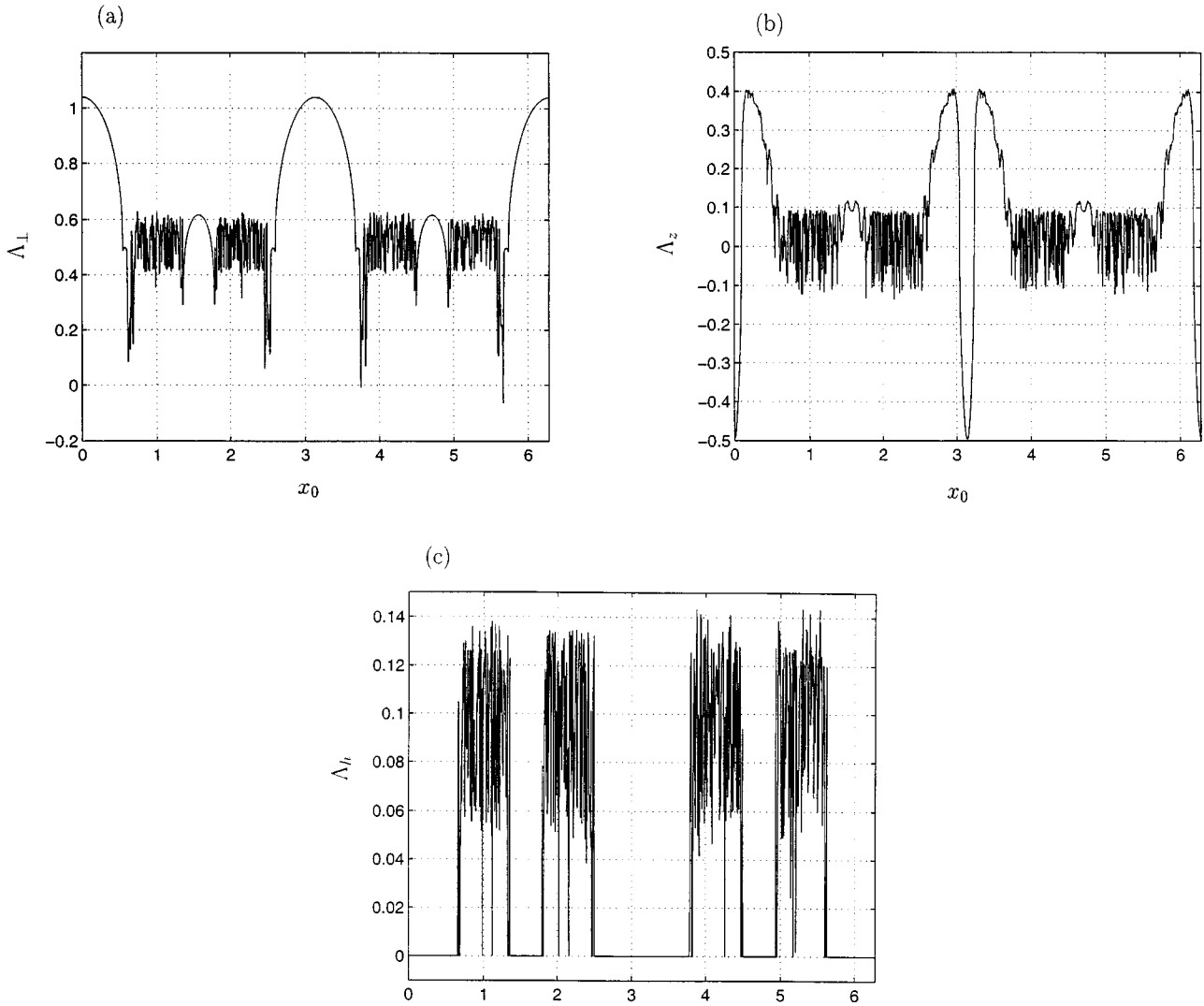


FIG. 1. For Eq. (4), the Lyapunov exponents versus the initial condition x_0 for $x_0 \in [0, 2\pi]$ ($y_0 = \pi$, $z_0 = 0.68$): (a) Λ_{\perp} versus x_0 , (b) Λ_z versus x_0 , and (c) Λ_h versus x_0 . The parameter setting is $k=1$ in the standard map, $a=3$, $b=0$, and $c=1$. The Lyapunov exponents show both smooth parts and wildly oscillating parts, corresponding to trajectories in the invariant plane on KAM surfaces and in chaotic components, respectively.

$$\begin{aligned} \Lambda_{\perp} &= \lim_{n \rightarrow \infty} \frac{1}{n} \sum_{j=1}^n \ln |a \cos x_j + b \cos y_j + c| \\ &= \int_0^{2\pi} (\ln |a \cos x_n + b \cos y_n + c|) \rho(x, y | x_0, y_0) dx dy, \end{aligned} \quad (5)$$

where $\rho(x, y | x_0, y_0)$ is the invariant density of x and y in the standard map for the trajectory starting from the initial condition (x_0, y_0) . The Lyapunov exponent of the transverse subspace Λ_T is

$$\Lambda_T = \Lambda_z \approx \Lambda_{\perp} + \int \ln |\cos(2\pi z_n)| \rho_z(z | x, y) dz, \quad (6)$$

where $\rho_z(z | x, y)$ is the invariant density of z under the x and y driving. We note that if $\Lambda_{\perp} < 0$, then $\Lambda_z = \Lambda_{\perp}$ because in this case the invariant (x, y) plane attracts points nearby. As

a consequence, z_n approaches zero asymptotically and the integral in Eq. (6) vanishes. In subsequent numerical experiments, we fix $a=3$, $b=0$, and $c=1$. To examine multiple coexisting attractors and their basin structures, we uniformly choose initial conditions from the one-dimensional line defined by $x_0 \in [0, 2\pi]$, $y_0 = \pi$, and $z_0 = 0.68$. For each initial condition, we compute Λ_{\perp} , Λ_z , and also $\Lambda_S = \Lambda_h$, the largest Lyapunov exponent for trajectories generated by the standard map in the invariant subspace. The computation is done by using 10^6 iterations and 10^6 preiterations. Note that since the dynamics in the invariant subspace is Hamiltonian, Λ_h must be non-negative: It is zero when the trajectory (x, y) falls on KAM surfaces and it is positive when the trajectory is in the chaotic component. Figures 1(a)–1(c) show Λ_{\perp} , Λ_z , and Λ_h versus x_0 . It can be seen that these plots contain both smooth parts and wildly oscillating parts. The smooth parts correspond to trajectories whose motion in x and y occurs on KAM islands and the values of Λ_h for these parts are zero [Fig. 1(c)]. The wildly oscillating parts correspond to trajec-

jectories in the chaotic component in the invariant plane. Since there are bounding KAM circles, different initial conditions generate characteristically different chaotic sets in the invariant plane, giving rise to different values of the Lyapunov exponents. For most initial conditions, Λ_{\perp} is always positive, indicating that the invariant plane (x,y) is repulsive in the transverse direction z for most initial conditions. This is due to the rather large value of a ($a=3$) used. Decreasing a can cause Λ_{\perp} to have both positive and negative values. From Fig. 1(b) we see that Λ_z can be either positive or negative. Thus, from Figs. 1(b) and 1(c), we see that depending on the initial condition, qualitatively different attractors in the full phase space (x,y,z) can be generated. These attractors can have (i) no positive Lyapunov exponent ($\Lambda_h=0$, $\Lambda_z<0$), (ii) one positive Lyapunov exponent ($\Lambda_h>0$, $\Lambda_z<0$, or $\Lambda_h=0$, $\Lambda_z>0$), and (iii) two positive Lyapunov exponents ($\Lambda_h>0$, $\Lambda_z>0$). In case (i), depending on the sign of Λ_{\perp} , there can be quasiperiodic attractors ($\Lambda_{\perp}<0$) or strange nonchaotic attractors ($\Lambda_{\perp}>0$). In the following, we discuss the dynamical mechanism for generating these different types of attractors.

A. Quasiperiodic attractors and strange nonchaotic attractors

For a given initial condition, if there are no positive Lyapunov exponents, both quasiperiodic attractors and strange nonchaotic attractors [16] can arise. Quasiperiodic attractors occur if (a) the initial condition (x_0, y_0) leads to a trajectory on a KAM surface in the invariant plane $z=0$ and (b) $\Lambda_{\perp}<0$ so that points in the transverse subspace are attracted towards $z=0$. Figure 2(a) shows such an attractor for $x_0=0.613$ in the phase space for which $\Lambda_{\perp}=\Lambda_z\approx-0.063$ and $\Lambda_h=0$. Clearly, the motion is confined to a period-2 torus in the (x,y) plane. Figure 2(b) shows the power spectrum computed from the time series y_n of 2^{15} trajectory points. This is a discrete power spectrum of the two-frequency quasiperiodic motion.

The more interesting case is the occurrence of strange nonchaotic attractors. These are attractors that are geometrically complicated, but trajectories on these attractors exhibit no sensitive dependence on initial conditions [16]. The word *strange* usually refers to the complicated geometry of the attractor: A strange attractor contains an uncountably infinite number of points and it is not piecewise differentiable. The word *chaotic* refers to a sensitive dependence on initial conditions: Trajectories originating from nearby initial conditions diverge exponentially in time. Strange nonchaotic attractors occur commonly in quasiperiodically driven dissipative dynamical systems [16]. We find that, in our case, strange nonchaotic attractor can arise when the trajectory in the (x,y) plane falls on a KAM surface but $\Lambda_{\perp}>0$ so that the invariant plane repels, transversely, points in its vicinity. Figures 3(a) and 3(b) show, for $x_0=0.541$, the (x,y) projection and the (x,z) projection of such an attractor, respectively. The values of the Lyapunov exponents are $\Lambda_z\approx-0.016$, $\Lambda_h=0$, and $\Lambda_{\perp}=0.485$. In this case, the (x,y) projection of the attractor is quasiperiodic [Fig. 3(a)], but the attractor appears to be strange in the (x,z) plane [Fig. 3(b)]. Since both Λ_z and Λ_h are nonpositive, the attractor is nonchaotic. Figure 3(c) shows the power spectrum of the time series z_n . The spectrum has the broad band-looking feature, in spite of the attractor's being nonchaotic, which is also typical of strange nonchaotic attractors [16].

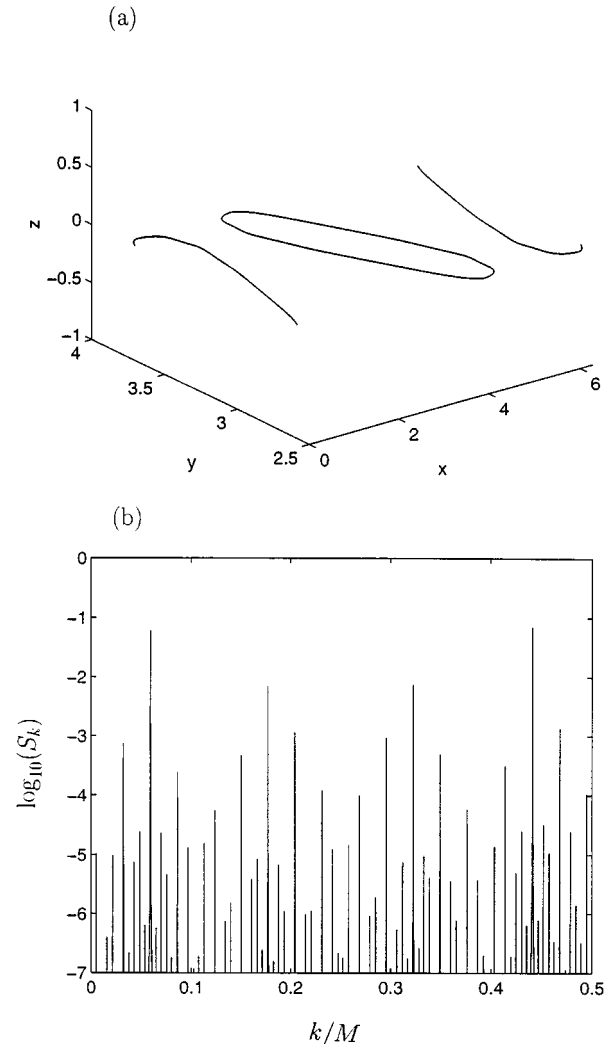


FIG. 2. For $x_0=0.613$ (a) the quasiperiodic attractor at $z=0$ and (b) the power spectrum of 2^{15} points from the time series y_n . The Lyapunov exponents are $\Lambda_{\perp}=\Lambda_z\approx-0.063$ and $\Lambda_h=0$. Note that $\Lambda_{\perp}<0$ so that z_n approaches zero asymptotically.

To understand how the quasiperiodic dynamics in the invariant plane gives rise to a strange nonchaotic attractor in the full phase space, we note that when $\Lambda_{\perp}>0$, the KAM surface in the invariant plane is *transversely unstable*. Consequently, there are time intervals during which a trajectory in the vicinity of $z=0$ is repelled away from it. In this case, if there are no other attractors in the phase space, the trajectory must return to the neighborhood of $z=0$ intermittently because the dynamics is bounded in z . Thus the asymptotic attractor in the full phase space exhibits a complicated geometric shape. But since Λ_z is negative, the attractor, though geometrically complex, is not chaotic. Thus a strange nonchaotic attractor is created [17].

B. Chaotic attractors with one positive Lyapunov exponent

There are two possibilities for generating chaotic attractors with one positive Lyapunov exponent.

Case (a): $\Lambda_h>0$ and $\Lambda_z<0$. This corresponds to the situation where the trajectory in the invariant plane is chaotic, but the z dynamics is not chaotic. Figures 4(a) and 4(b)

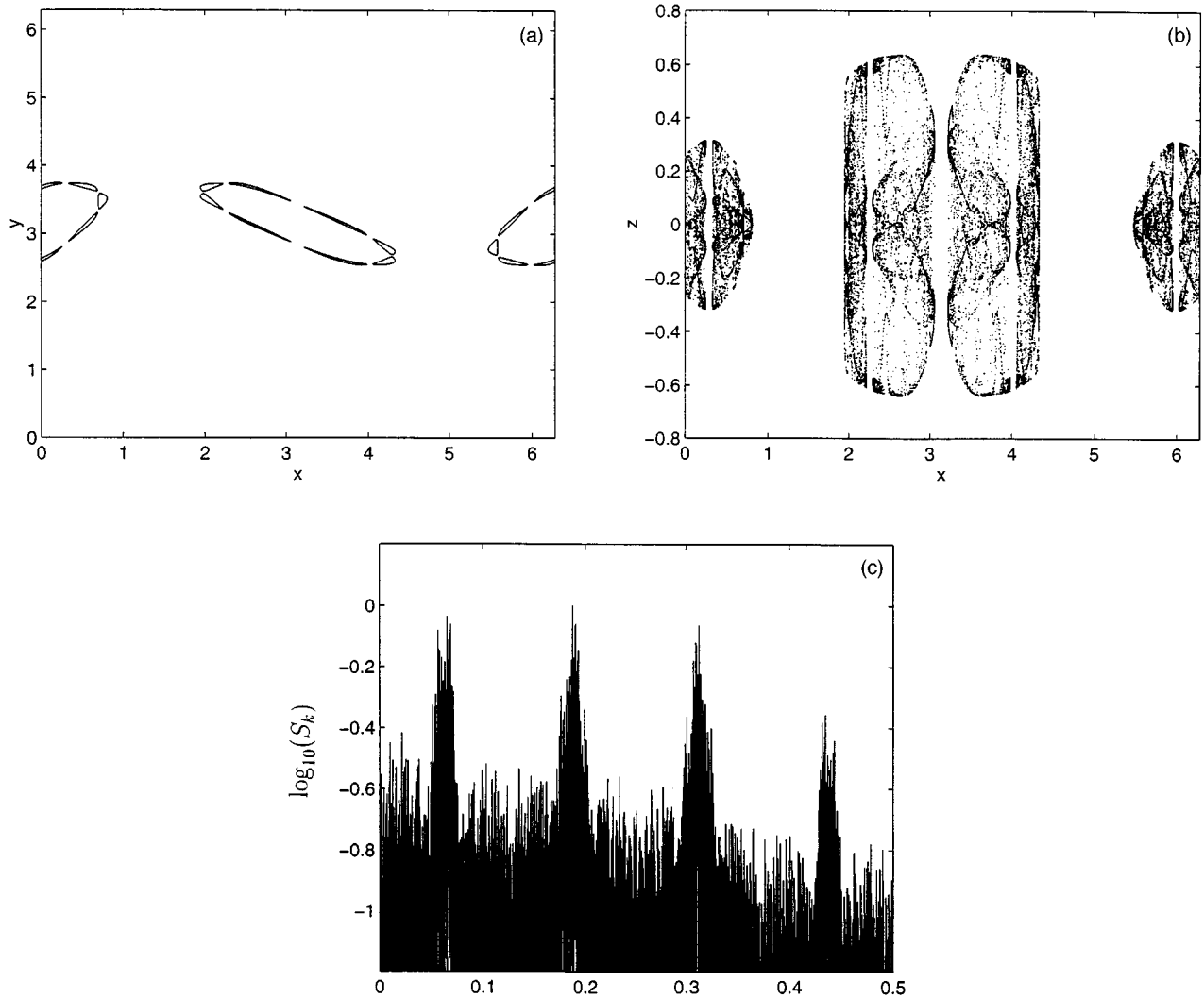


FIG. 3. For $x_0=0.541$ (strange nonchaotic attractor) (a) the corresponding quasiperiodic motion in the invariant plane (x,y) , (b) the projection of the attractor onto the (x,z) plane, and (c) the power spectrum of the time series z_n . The Lyapunov exponents are $\Lambda_{\perp} \approx 0.485$, $\Lambda_z \approx -0.016$, and $\Lambda_h = 0$. Strange nonchaotic attractor arises because $\Lambda_{\perp} > 0$, but $\Lambda_z < 0$ (see the text).

show, for $x_0=0.904$, the (x,y) projection and the (x,z) projection of such an attractor. It can be seen that the (x,y) projection of the attractor fills a chaotic layer of the Hamiltonian phase space in the invariant plane [Fig. 4(a)]. The two Lyapunov exponents are $\Lambda_h \approx 0.063$ and $\Lambda_z \approx -0.099$. The Lyapunov dimension [18] of the attractor is thus between 2 and 3. The transverse Lyapunov exponent is $\Lambda_{\perp} \approx 0.418$. Since Λ_{\perp} is positive, points in the vicinity of the invariant plane can be repelled away from it and hence the attractor spreads into both the positive and negative z directions, as shown in Fig. 4(b). The reason why Λ_{\perp} is positive but Λ_z is negative can be understood by noting that the integral in Eq. (6) is always negative. Thus, in general, we have $\Lambda_z < \Lambda_{\perp}$ and hence it is possible to have $\Lambda_{\perp} > 0$ and $\Lambda_z < 0$. The power spectrum of this attractor has a broadband feature, as shown in Fig. 4(c).

Case (b): $\Lambda_h = 0$ and $\Lambda_z > 0$. In this case, the motion in the invariant plane is quasiperiodic, but the quasiperiodic driving generates sensitive dependence on initial conditions in the transverse z direction. Figures 5(a) and 5(b) show, respectively, the (x,y) projection and the (x,z) projection of such

an attractor for $x_0=0.634$, where the Lyapunov exponents are $\Lambda_h = 0$ and $\Lambda_z \approx 0.024$. Thus the Lyapunov dimension of the attractor is 2. The transverse Lyapunov exponent is $\Lambda_{\perp} \approx 0.243$. The quasiperiodic motion in the invariant plane is evident, as can be seen in Fig. 5(a). Note the similarity between Figs. 5(b) and 3(b) as both are generated by quasiperiodic driving in the invariant plane. In fact, the chaotic attractor in Fig. 5 develops from strange nonchaotic attractors at smaller value of the parameter a . This was verified by fixing the initial condition x_0 and examining Λ_{\perp} and Λ_z as a increases from $a=1$. The power spectrum of the time series z_n exhibits a broadband feature that is typical of chaotic attractors, as shown in Fig. 5(c).

C. Chaotic attractors with two positive Lyapunov exponents

This type of chaotic attractors is generated by chaotic trajectories in the invariant plane. Usually, the transverse Lyapunov exponent has large positive values. The invariant density $\rho_z(z|x,y)$ generated leads to a small negative value for the integral in Eq. (6) so that Λ_z is positive. Figures 6(a)

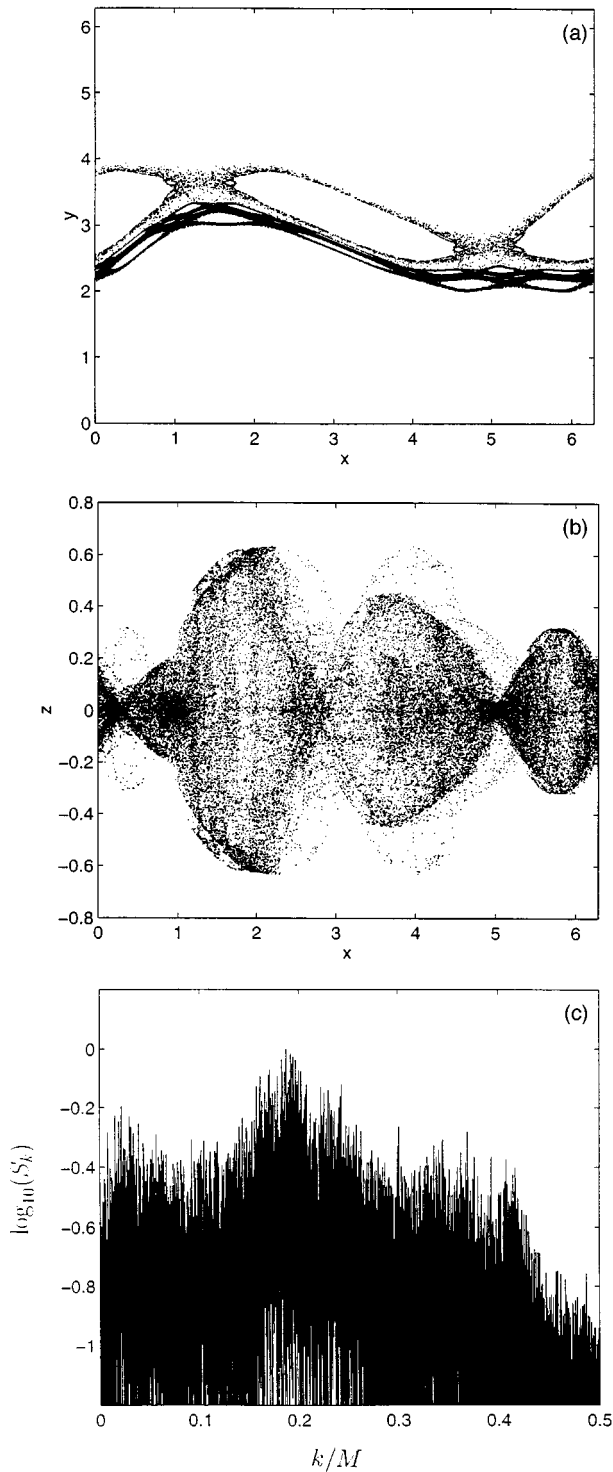


FIG. 4. For $x_0=0.904$ (chaotic attractor with one positive Lyapunov exponent) (a) the corresponding chaotic motion in the invariant plane (x,y) , (b) the projection of the attractor onto the (x,z) plane, and (c) the power spectrum of the time series z_n . The Lyapunov exponents are $\Lambda_{\perp} \approx 0.418$, $\Lambda_z \approx -0.099$, and $\Lambda_h \approx 0.063$. In this case, the motion in the invariant plane is chaotic, but the z Lyapunov exponent is negative.

and 6(b) show, for $x_0=0.832$, the (x,y) projection and the (x,z) projection of such an attractor, respectively. The Lyapunov exponents are $\Lambda_h \approx 0.133$, $\Lambda_z \approx 0.083$, and $\Lambda_{\perp} \approx 0.603$. The Lyapunov dimension of the attractor is be-

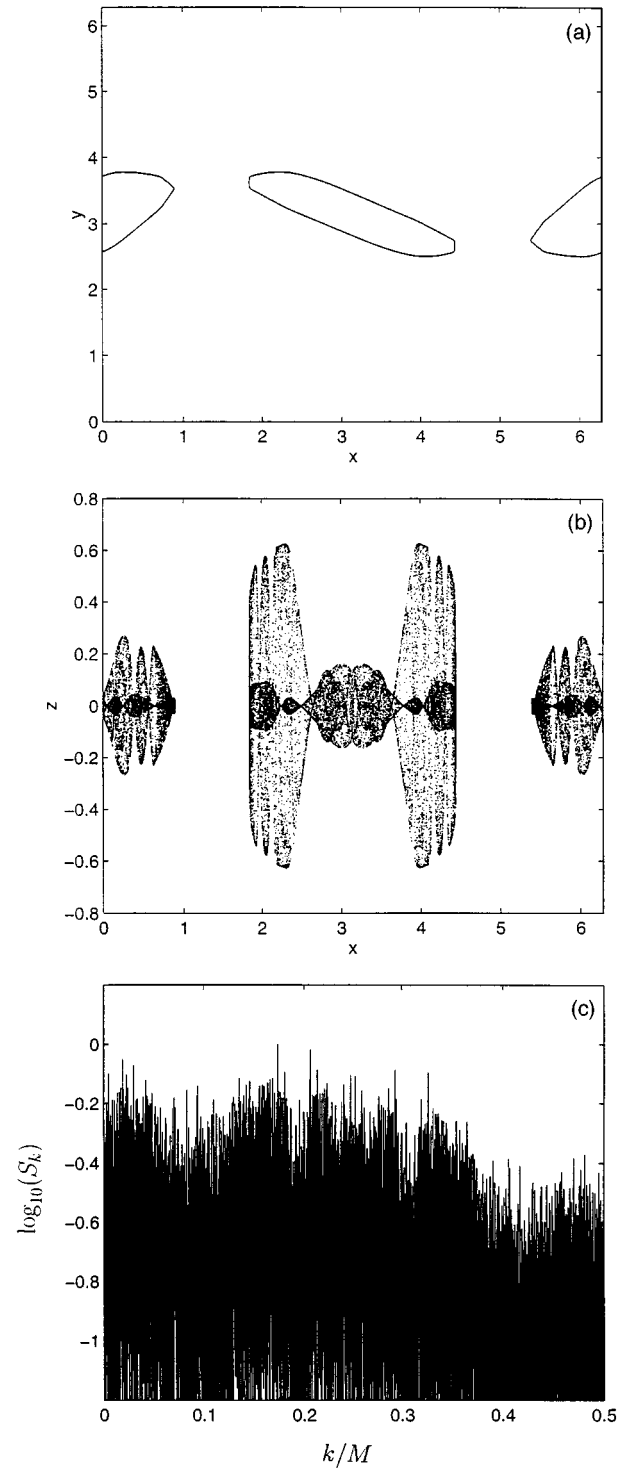


FIG. 5. For $x_0=0.634$ (chaotic attractor with one positive Lyapunov exponent) (a) the corresponding quasiperiodic motion in the invariant plane (x,y) , (b) the projection of the attractor onto the (x,z) plane, and (c) the power spectrum of the time series z_n . The Lyapunov exponents are $\Lambda_{\perp} \approx 0.243 > 0$, $\Lambda_z \approx 0.024 > 0$, and $\Lambda_h = 0$. Note that the chaotic attractor is generated by a quasiperiodic driving in the invariant plane.

tween 2 and 3. This type of hyperchaotic attractor is usually created when the trajectory in the invariant plane is in a large chaotic component [19], as can be seen in Fig. 6(a). The power spectrum of the time series z_n is shown in Fig. 6(c), which has a broadband feature.

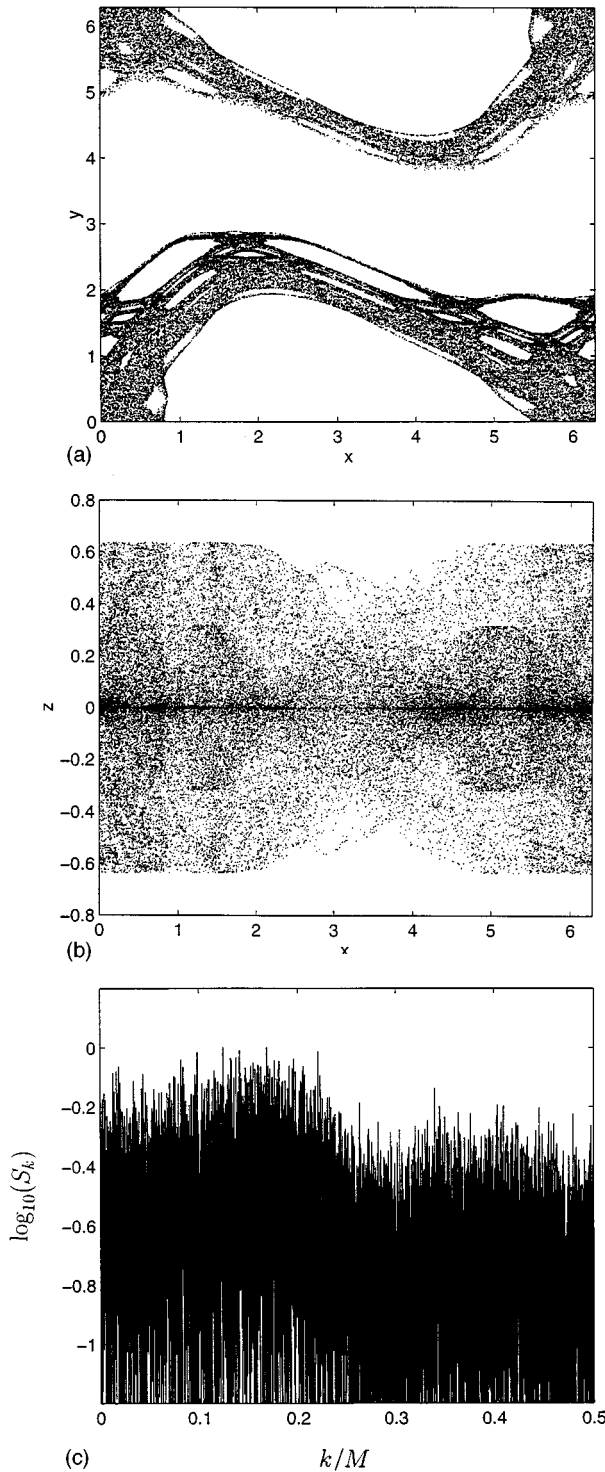


FIG. 6. For $x_0=0.832$ (chaotic attractor with two positive Lyapunov exponents) (a) the corresponding chaotic motion in the invariant plane (x, y) , (b) the projection of the attractor onto the (x, z) plane, and (c) the power spectrum of the time series z_n . The Lyapunov exponents are $\Lambda_\perp \approx 0.603$, $\Lambda_z \approx 0.083$, and $\Lambda_h \approx 0.133$. In this case, the motion in the invariant plane is chaotic and the z Lyapunov exponent is also positive.

IV. FINAL-STATE SENSITIVITY AND THE UNCERTAINTY EXPONENTS

The wild oscillation of the Lyapunov exponents in Figs. 1(a)–1(c) as the initial condition varies continuously along a

straight line in the invariant plane indicates that the asymptotic attractor of the system depends sensitively on the initial condition: A small change in the initial condition may lead to qualitatively different attractors. This is the so-called *final-state sensitivity* [12]. An implication is that the basins of attraction of various coexisting chaotic and nonchaotic attractors are interwoven in a complicated way.

The final-state sensitivity can be quantified by the uncertainty exponent [12]. Suppose that we choose a random initial condition x_0 and apply a small perturbation ϵ to it to get another nearby initial condition $x_0 + \epsilon$. Since, obviously, there is an infinite number of attractors [Figs. 1(b) and 1(c)], small perturbations would lead to either a completely different type of attractor with Lyapunov exponents of different sign or a similar attractor with Lyapunov exponents only differing in magnitude but not in sign. Our goal is to assess, numerically, whether small perturbations can lead to qualitatively different attractors. Thus we compute the Lyapunov exponents Λ_z and Λ_h for both initial conditions x_0 and $x_0 + \epsilon$. For simplicity, we distinguish three cases: (i) $\Lambda_z > 0$ and $\Lambda_h > 0$ (two positive exponents); (ii) $\Lambda_z > 0$ and $\Lambda_h = 0$, or $\Lambda_z < 0$ and $\Lambda_h > 0$ (one positive exponent); and (iii) $\Lambda_z < 0$ and $\Lambda_h < 0$ (no positive exponent). If x_0 and $x_0 + \epsilon$ lead to Lyapunov exponents belonging to these different cases, we say that the initial condition x_0 is *uncertain with respect to the perturbation* ϵ . For fixed ϵ , a large number of random initial conditions can be chosen to yield the fractions of the uncertain initial conditions. Specifically, choose N_T (large) initial conditions. Let $N_{21}(\epsilon)$ be the number of initial conditions that are uncertain between case (i) and case (ii) (two positive Lyapunov exponents versus one positive Lyapunov exponent) and let $N_{210}(\epsilon)$ be the number of uncertain initial conditions between case (i) or (ii) and case (iii) (chaotic versus nonchaotic). The corresponding uncertain fractions are $f_{21}(\epsilon) \approx N_{21}/N_T$ and $f_{210}(\epsilon) \approx N_{210}/N_T$. In general, $f_{12}(\epsilon)$ and $f_{120}(\epsilon)$ scale with ϵ algebraically,

$$f_{21}(\epsilon) \sim \epsilon^{\alpha_{21}}, \quad f_{210}(\epsilon) \sim \epsilon^{\alpha_{210}}, \quad (7)$$

where the non-negative scaling exponents α_{21} and α_{210} are called the uncertainty exponents. Such algebraic scaling relations have been argued for general dynamical systems in Ref. [12] and have been rigorously proven for axiom-A systems in Ref. [20].

Figures 7(a) and 7(b) show $f_{21}(\epsilon)$ and $f_{210}(\epsilon)$ versus ϵ on a logarithmic scale, where initial conditions are chosen from the same one-dimensional line used to compute Figs. 1(a)–1(c). In the computation, we increase N_T until N_{21} reaches 500 to obtain $f_{21}(\epsilon)$ and $f_{210}(\epsilon)$. The uncertainty exponents are $\alpha_{21} \approx 0.0$ and $\alpha_{210} = 0.42 \pm 0.05 > 0$. These different values of the uncertainty exponents have significant consequences regarding predictability of the asymptotic attractor of the system. In particular, regard ϵ as the error in specifying the initial condition x_0 . The fact that α_{21} cannot be distinguished from zero indicates that $f_{21}(\epsilon)$ does not decrease appreciably even when ϵ is decreased by many orders of magnitude. This implies the worst case of predictability: It is impossible to predict, *for specific initial conditions*, whether the attractor has two positive Lyapunov exponents or one positive exponent. However, the situation is improved if one attempts to predict whether the attractor is chaotic or nonchaotic because

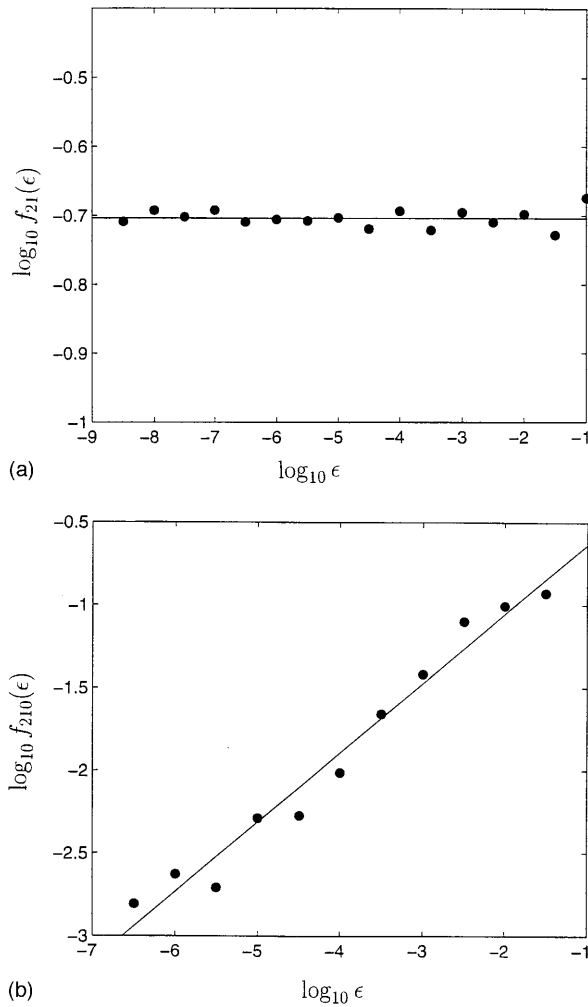


FIG. 7. Uncertain fractions (a) $f_{21}(\epsilon)$ and (b) $f_{210}(\epsilon)$ versus ϵ on a logarithmic scale. The uncertainty exponents are $\alpha_{21} \approx 0.0$ and $\alpha_{210} \approx 0.42$. Since α_{21} cannot be distinguished from zero, it is practically impossible to predict whether the attractor has one or two positive Lyapunov exponents. However, since α_{210} is finite, it is possible to distinguish chaotic attractors from nonchaotic ones if initial conditions and parameters are specified with sufficient precision (see the text).

α_{210} has a finite value of about 0.42. For instance, when $\epsilon = 10^{-1}$, we have $f_{210}(\epsilon) \sim 0.4$. In order to reduce $f_{210}(\epsilon)$ to, say, 10^{-3} , one needs to reduce ϵ to about 10^{-9} . Although a decrease in ϵ does not yield an equal decrease in $f_{210}(\epsilon)$, the situation is better than the one with $f_{21}(\epsilon)$ that does not decrease regardless of how much ϵ is decreased. The reason that $\alpha_{210} > 0$ is directly related to the Hamiltonian phase-space structure in the invariant plane. Note that nonchaotic attractors must be generated by trajectories falling on KAM surfaces in the invariant plane. It is believed that the set of phase-space regions occupied by the chaotic components is a fat fractal, i.e., a fractal with a positive Lebesgue measure [21]. Thus, if an initial condition yields a chaotic trajectory in the invariant plane, a small perturbation to the initial condition can yield a quasiperiodic trajectory on the KAM surface. But for an initial condition that yields a trajectory on the KAM surface, small perturbation always produce trajectories that are still on the KAM surfaces.

V. DISCUSSION

In this paper we have introduced a class of low-dimensional dynamical systems that exhibit extremely rich complex behavior. The system is a mixture of Hamiltonian and dissipative dynamics, where the Hamiltonian dynamics occurs in some invariant subspace of the system and the dissipation occurs in the transverse subspace. The dynamics in the full phase space is thus dissipative and, for typical initial conditions, the asymptotic sets can be attractors. We demonstrate that this class of systems exhibits all three traits characterizing a complex system. In particular, for typical parameter values, a variety of distinct attractors coexist. These are quasiperiodic attractors, strange nonchaotic attractors, and chaotic attractors with different number of positive Lyapunov exponents. The basins of these attractors appear to be interwoven in a complicated manner. As a consequence, the qualitative prediction of even the type of the asymptotic attractor for specific initial conditions and parameters becomes extremely difficult. We remark that Hamiltonian dynamics is common in physical systems, but small friction is inevitable. Our work thus demonstrates that the combination and interplay of conservative and dissipative dynamics can lead to complex behavior even for physical systems with a few degrees of freedom.

Recent work by Feudel *et al.* [11] demonstrated that complexity can arise in the weakly dissipative standard map. Due to the weak dissipation, the original elliptic periodic orbits become small sinks and hence an infinite number of periodic attractors can coexist. It was found that the basins of these sinks are usually interwoven in a complicated way. We should mention that our system is quite different from Hamiltonian systems with weak dissipation. In the latter case, the system itself is weakly dissipative and there is no Hamiltonian component in the system. In contrast, our system has Hamiltonian dynamics in the invariant subspace and the dissipation can be strong and it occurs in the transverse direction. While the observed complexity in our system is a direct consequence of the Hamiltonian phase-space structure that typically contains chaotic components and hierarchies of KAM islands, we see that the introduction of dissipation in the transverse direction gives rise to much richer complexity. Quasiperiodic motion on KAM surfaces in the invariant subspace can lead to quasiperiodic, strange nonchaotic, and chaotic attractors in the full phase space. Chaotic motion in the invariant subspace can induce chaotic attractors with different numbers of positive Lyapunov exponents. Thus the rich complexity observed in this paper is a *nontrivial* manifestation of the invariant Hamiltonian dynamics in the full phase space.

ACKNOWLEDGMENTS

This work was supported by the Department of Energy (Mathematical, Information and Computational Sciences Division, High Performance Computing and Communication Program). The numerical work was supported by a grant from the W. M. Keck Foundation through the University of Maryland. Y. C. L. was supported by the Air Force Office of Scientific Research, Air Force Material Command, USAF, under Grant No. F49620-96-1-0066. Y. C. L. was also supported by the General Research Fund at the University of Kansas, and by the K* STAR NSF EPSCoR Program in Kansas.

- [1] R. Badii and A. Politi (unpublished); in *Measures of Complexity*, edited by L. Peliti and A. Vulpiani (Springer-Verlag, Berlin, 1988).
- [2] J. P. Crutchfield and K. Young, *Phys. Rev. Lett.* **63**, 105 (1989).
- [3] P. Grassberger, in *Fifth Mexican School on Statistical Mechanics*, edited by F. Ramos-Gómez (World Scientific, Singapore, 1991).
- [4] R. Badii, in *Chaotic Dynamics: Theory and Practice*, edited by T. Bountis (Plenum, New York, 1992).
- [5] L. Poon and C. Grebogi, *Phys. Rev. Lett.* **75**, 4023 (1995).
- [6] P. Bergé and M. Dubois, *Phys. Lett.* **93A**, 365 (1983).
- [7] P. E. Rapp *et al.*, *J. Neurosci.* **14**, 4731 (1994).
- [8] F. T. Arecchi, G. Giacomelli, P. L. Ramazza, and S. Residori, *Phys. Rev. Lett.* **65**, 2531 (1990).
- [9] C. S. Daw, C. E. A. Finney, M. Vasudevan, N. A. van Goor, K. Nguyen, D. D. Bruns, E. J. Kostelich, C. Grebogi, E. Ott, and J. A. Yorke, *Phys. Rev. Lett.* **75**, 2308 (1995).
- [10] C. Grebogi, E. J. Kostelich, E. Ott, and J. A. Yorke, *Physica D* **25**, 347 (1987); F. Romeiras, C. Grebogi, E. Ott, and W. P. Dayawansa, *ibid.* **58**, 165 (1992); S. Dawson, C. Grebogi, T. Sauer, and J. A. Yorke, *Phys. Rev. Lett.* **73**, 1927 (1994).
- [11] U. Feudel, C. Grebogi, B. Hunt, and J. A. Yorke, *Phys. Rev. E* **54**, 71 (1996).
- [12] C. Grebogi, S. W. McDonald, E. Ott, and J. A. Yorke, *Phys. Lett.* **99A**, 415 (1983); S. W. McDonald, C. Grebogi, E. Ott, and J. A. Yorke, *Physica D* **17**, 125 (1985).
- [13] K. T. Alligood, T. Sauer, and J. A. Yorke, *Chaos: An Introduction to Dynamical Systems* (Springer-Verlag, New York, 1996).
- [14] A. J. Lichtenberg and M. A. Leiberman, *Regular and Chaotic Dynamics* (Springer-Verlag, New York, 1992).
- [15] J. C. Alexander, J. A. Yorke, Z. You, and I. Kan, *Int. J. Bifur. Chaos* **2**, 795 (1992); I. Kan, *Bull. Am. Math. Soc.* **31**, 68 (1994); E. Ott, J. C. Alexander, I. Kan, J. C. Sommerer, and J. A. Yorke, *Physica D* **76**, 384 (1994); J. F. Heagy, T. L. Carroll, and L. M. Pecora, *Phys. Rev. Lett.* **73**, 3528 (1994); P. Ashwin, J. Buescu, and I. N. Stewart, *Phys. Lett. A* **193**, 126 (1994); Y. C. Lai and C. Grebogi, *Phys. Rev. E* **52**, R3313 (1995).
- [16] C. Grebogi, E. Ott, S. Pelikan, and J. A. Yorke, *Physica D* **13**, 261 (1984); F. J. Romeiras and E. Ott, *Phys. Rev. A* **35**, 4404 (1987); F. J. Romeiras, A. Bondeson, E. Ott, T. M. Antonsen, Jr., and C. Grebogi, *Physica D* **26**, 277 (1987); M. Ding, C. Grebogi, and E. Ott, *Phys. Rev. A* **39**, 2593 (1989); W. L. Ditto, M. L. Spano, H. T. Savage, S. N. Rauseo, J. F. Heagy, and E. Ott, *Phys. Rev. Lett.* **65**, 533 (1990); T. Zhou, F. Moss, and A. Bulsara, *Phys. Rev. A* **45**, 5394 (1992); J. F. Heagy and S. M. Hammel, *Physica D* **70**, 140 (1994); A. S. Pikovsky and U. Feudel, *Chaos* **5**, 253 (1995); *J. Phys. A* **27**, 5209 (1994); U. Feudel, J. Kurths, and A. S. Pikovsky, *Physica D* **88**, 176 (1995); S. P. Kuznetsov, A. S. Pikovsky, and U. Feudel, *Phys. Rev. E* **51**, R1629 (1995); Y. C. Lai, *ibid.* **53**, 57 (1996).
- [17] T. Yalcinkaya and Y. C. Lai (unpublished).
- [18] J. L. Kaplan and J. A. Yorke, in *Functional Differential Equations and Approximations of Fixed Points*, edited by H.-O. Peitgen and H.-O. Walter, *Lecture Notes in Mathematics Vol. 730* (Springer, Berlin, 1979).
- [19] A common feature of Hamiltonian systems is the stickiness effect of KAM islands. The Lyapunov exponent for trajectories on a KAM surface is zero. The symplectic nature of the Hamiltonian dynamics stipulates that the Lyapunov exponent in the direction transverse to the KAM surface is also zero. When a trajectory in the surrounding chaotic component comes close to the KAM surface, it can spend a long time in the vicinity of the KAM surface. Different chaotic regions are connected through the Cantori after the breakup of KAM surfaces. Thus a chaotic trajectory usually spends a long time in some phase-space region near some KAM surface before crossing the Cantori and spending a long time in another distinct chaotic region. Since the Lyapunov exponents Λ_{\perp} , Λ_z , and Λ_h are determined by the trajectory in the invariant subspace, we see that the values of these exponents may change when different numbers of iterations are used in the computation. Thus, asymptotically, some chaotic attractors with one or two positive Lyapunov exponents may belong to the same category. Nonetheless, from a practical point of view, in a finite time scale one can still distinguish between attractors generated by chaotic trajectories in the invariant subspace. We use 2×10^6 iterations to compute these Lyapunov exponents. Hence the attractors are distinct for at least 2×10^6 iterations. On the other hand, there is no ambiguity when one distinguishes between attractors produced by quasiperiodic trajectories on the KAM surfaces and by chaotic trajectories in the invariant subspace. For stickiness effect and the concept of Cantori, see R. S. MacKay, J. D. Meiss, and I. C. Percival, *Physica D* **13**, 55 (1984); **27**, 1 (1987); J. D. Meiss and E. Ott, *ibid.* **20**, 387 (1986); *Hamiltonian Dynamical Systems: A Reprint Selection*, edited by R. S. MacKay and J. D. Meiss (Hilger, Bristol, 1987).
- [20] C. Grebogi, H. E. Nusse, E. Ott, and J. A. Yorke, in *Dynamic Systems*, edited by J. A. Alexander, *Lecture Notes in Mathematics Vol. 1342* (Springer-Verlag, New York, 1988).
- [21] D. K. Umberger and J. D. Farmer, *Phys. Rev. Lett.* **55**, 661 (1985).